19

Protein-DNA Interactions Studies with Single Tethered Molecule Techniques

Guy Nir, Moshe Lindner and Yuval Garini
Physics Department and institute of Nanotechnology,
Bar Ilan University, Ramat Gan,
Israel

1. Introduction

The last decade has seen a leap forward in the understanding of molecular and cellular mechanisms with the development of advanced techniques for observing, manipulating and imaging single molecules. In contrast to conventional biochemical techniques which yield information derived from population averages, single molecule techniques give access to the dynamics and properties of individual biomolecules in situ.

One of the problems in studying single molecules is the need to observe and measure the molecule for a large enough period of time and hence different approaches were developed. Among the various experimental single molecule techniques, one of the most convenient to implement is Tethered Particle Motion (TPM) (Schafer, Gelles *et al.* 1991; Nelson, Zurla *et al.* 2006; Zurla, Franzini *et al.* 2006; Jeon & Metzler 2010). In the most common procedure of TPM approach, a bead is attached to the DNA in one end, while the other end is immobilized to a glass surface (Figure 1). The Brownian motion of the nano-bead can be imaged through a microscope with an array detector such as a charged coupled detector (CCD) camera that captures the position of the bead in time and space. The bead positions are analyzed by using single particle motion (SPT) algorithms and its distribution is calculated. It is directly related to the expected conformations of the DNA when it is treated as a polymer with a given nominal length and stiffness.

The DNA contains a long chain of nucleic acids that contains all of our genetic information and a stretched human DNA molecule is about 2 meters long. This long molecule is divided to 46 chromosomes (in human cells) that are packed into a human cell that is only 10-100 μm large, which necessitates that the DNA structure will be highly regulated. Moreover, the DNA packaging has to ensure the appropriate functioning of the DNA-related processes such as transcription and replication.

All the processes that involve DNA, mainly remodeling, transcription and replication, are performed by a set of proteins that interact with the DNA in different ways. Therefore, these proteins are crucial and the understanding of their interaction patterns with the DNA is of great interest. DNA-protein interactions are therefore a subject of an ongoing research mediated by different methodologies. Better understanding of the interaction mechanisms

could lead to new diagnostics methods, the discovery of new drug targets and altogether can affect mankind health.

The mechanisms described above can be studied with single molecule techniques in great details and provide information that in many cases is undetectable when using ensemble techniques. One example is the motor enzymes, such as myosin V and kinesin, that proceed in nanometric steps (Yildiz, Forkey *et al.* 2003; Yildiz, Tomishige *et al.* 2004). A detailed description of their translocation mechanism requires labeling and tracking of single enzymes in high accuracy. Observing single labeled biomolecules avoids large-population averaging and allows deciphering each step-size. It also allows distinguishing transient kinetic steps in a multistep reaction and identifying rare or short-lived conformational states.

In this book chapter we will:

1. Describe single tethered-molecule detection methods that can be used for DNA-protein studies while emphasizing Tethered Particle Motion (TPM).
2. Review few key findings on relevant proteins.
3. Compare and summarize the method presented here.
4. Provide a fascinating glance to the dazzling near-future capabilities which are based on immerging single molecule detection methods for studying DNA-protein interactions.

2. Single tethered-molecule detection methods for DNA-protein studies

Recent progress in technology, especially in the fields of photonics and nanotechnology and their combination together with the profound knowledge obtained during the last decades in molecular biology has enabled the development of single-molecule applications. Here we will describe the following well-established methods: TPM, magnetic tweezers, optical tweezers, AFM and FRET. These methods have been used to perform cutting-edge experiments as we will show later in this chapter.

2.1 Tethered particle motion

2.1.1 General description of the method

TPM is an optical method that relies on physical models and biochemical approaches to detect and observe biophysical properties, such as the dynamic variations in conformations induced by enzymes acting on biopolymers. In TPM, the biopolymer of interest, i.e. linear double-stranded DNA (dsDNA), is attached at one end to a glass surface and hence held fixed, while the other end is labeled with a marker that can be a fluorescent tag or a metal bead and is free to diffuse in a restricted volume due to the anchoring of the other end (Figure 1). The bead positions that reflect the end-to-end distance of the biopolymer are recorded at different time-intervals and are than analyzed according to physical models to retrieve biophysical properties of the biopolymer, the enzymes acting on it and the nature of their interactions. One advantage of the method relies in the fact that unlike other single molecule techniques, TPM is a force-free technique, meaning that no external force is used to alter the studied molecules natural structure, which might lead to a more reliable measurement.

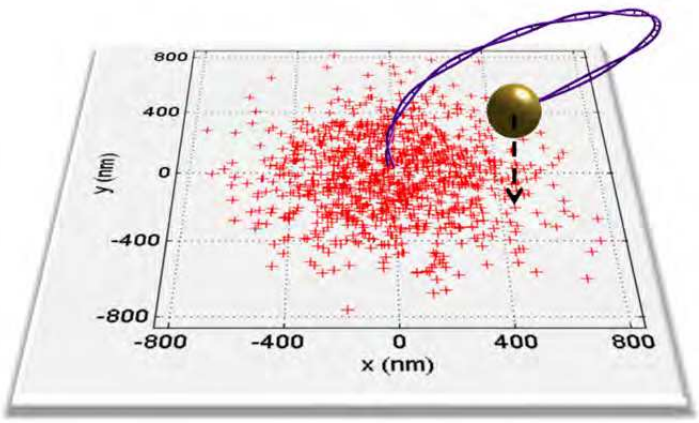

Fig. 1. TPM principles. A small bead is attached to one end of a polymer while its other end is attached to the surface. The bead performs Brownian motion in the solution constrained by the polymer. The bead positions (red crosses) are measured with an optical setup with an accuracy of few nanometers.

2.1.2 Physical model

Many biological processes such as replication, transcription and gene regulation require accessibility to the DNA. The DNA's contour in cells is regulated by DNA-bending proteins such as histones in eukaryotic cells (Shin, Santangelo *et al.* 2007) or histone-like proteins in prokaryotic cells (Rouviere-Yaniv 1987). Other proteins can bind or interact with the DNA and can modify its mechanical properties. Such interactions might alter the conformation of the DNA. TPM can detect such changes, but because they are not being measured directly, but only through the end-to-end distribution (as depicted from the bead measurement), it is necessary to use a model that describes the dependence of the DNA conformation on its basic physical parameters in space.

The DNA is known to be a rather stiff polymer that can be described to a good accuracy by the Worm-like-Chain (WLC) model. WLC is derived from the equivalent Freely Jointed Chain (FJC). The equivalent chain described by the model has the same mean square end-to-end distance $\langle R^2 \rangle$ and the same contour length, L, as the actual polymer, but it is described by N freely jointed effective bonds of length b (figure 2). This effective bond length b, is called Kuhn length. Accordingly we can write:

$$Nb = L \tag{1}$$

and its mean square end-to-end distance is

$$\langle R^2 \rangle = Nb^2 = bL \ . \tag{2}$$

Actually, one conventionally defines a ``persistence length'', l_p, in terms of how rapidly the direction of the polymer changes as a function of the contour length. Let us define the angle θ between a vector that is tangent to a certain polymer element and a tangent vector at a distance L along the polymer. It can be shown that the expectation value of the cosine of the angle falls off exponentially with distance,

$$\langle \cos\theta \rangle = e^{-L/l_p} \tag{3}$$

where the triangular brackets denote the average over all starting polymer-element positions. For DNA, the persistence length is twice the Kuhn length.

According to the WLC theory, for "naked" (proteins-free) double stranded DNA,

$$\langle R^2 \rangle \cong 2l_p L = bL \quad \text{for} \quad L >> l_p \,. \tag{4}$$

The persistence length of DNA in normal conditions is equal to 50 nm (Rubinstein & Colby 2003). If the polymer is free to assume any configuration in three dimensions, it can be shown that the probability distribution function (PDF) for its projection length along one-dimension (x or y axis) is a Gaussian:

$$P_{1D}(x)dx = \sqrt{\frac{3}{4\pi L l_p}} \cdot \exp\left(-\frac{3x^2}{4Ll_p}\right)dx \,. \tag{5}$$

The PDF of the two-dimensional projection length of the polymer on a plane in Polar coordinates can also be calculated and it is found to be the Rayleigh distribution:

$$P_{2D}(r)dr = \frac{3}{4\pi L l_p} \cdot \exp\left(-\frac{3r^2}{4Ll_p}\right) \cdot 2\pi r \cdot dr \tag{6}$$

where $r = \sqrt{x^2 + y^2}$.

Although real polymer chains are subjected to self-avoidance, meaning that due to short range repulsive forces, monomers of the chain can't cross themselves which leads to an excluded volume, it is accustomed to treat DNA molecules as ideal chains (also called phantom polymers), since the probability of crossing is non negligible only for long DNA (>40 μm) (Strick, Allemand *et al.*), which are not usually used in single-molecule experiments (Slutsky 2005).

2.1.3 Marker considerations

The DNA conformation changes randomly in the solution and its end-to-end distance is measured in TPM by finding the position of the attached marker. Different types of markers can be used and with respect to their detection method, one can distinguish fluorescent beads, scattering beads and beads that are detected by normal transmission or contrast enhancement methods. A fluorescent marker might be small but suffers from quenching and bleaching and is not recommended for long-time observations. Polystyrene microspheres

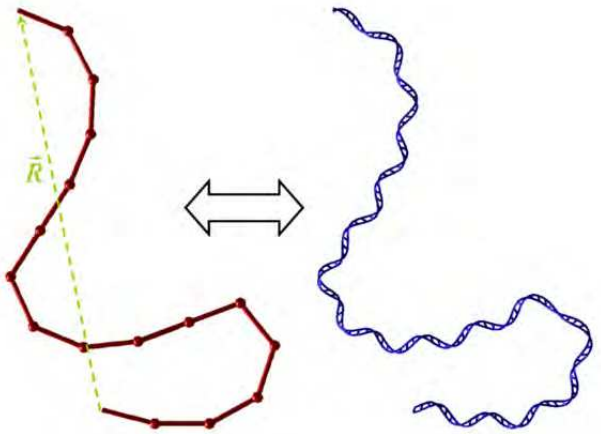

Fig. 2. Left: FJC model. Each segment is equal to b, the Kuhn length (~100 nm). $\vec{R}$ is the end-to-end vector. A real dsDNA is shown on the right and it is equivalent to the polymer in the FJC model.

are also used as markers normally with phase contrast microscopy, but it requires a rather large micron-size particle, which may lead to inaccurate analysis in TPM. If the size is too large, the measured position of the bead may be dominated by the free rotation of the marker around its tethering point. This motion is also affected by the position of the bead with respect to the surface, and therefore, the measured distribution may be dominated or severely influenced by the marker size. This will lead to errors when trying to extract the polymer properties from the bead distribution, and the bead-size effect cannot be easily compensated for. It is therefore better to work with smaller beads. The actual size that does not affect the distribution depends on the polymer contour length and persistence length. The problem was treated intensively in the literature (Segall, Nelson *et al.* 2006), and it was shown that the bead size will not affect the distribution significantly, as long as the parameter called the excursion number, is smaller than unity:

$$N_r = R / \sqrt{Ll_p / 3} < 1 . \tag{7}$$

The excursion number is defined as the ratio of the marker radius R to the radius of gyration of DNA which depends on the polymer persistence length l_p and contour length L.

Therefore, it is better to use a smaller bead size, and a more suitable solution is a small metal nano-bead. Such a bead has a significant plasmon scattering which results in an intense signal that can be easily detected by a CCD.

For DNA with a contour length of $L = 925nm$, a known persistence length of $l_p = 50nm$ for bare DNA and a gold bead with $r = 40$ nm gives $N_r \sim 0.32$ which meets the criterion (Segall, Nelson et al. 2006; Lindner, Nir et al. 2009).

Another advantage is the short exposure time that can be used, which still achieving a high-enough signal to noise for analyzing the bead position. If the exposure-time is too long, the bead motion broadens the image spot and the analyzed distribution of the bead position is skewed. Although this effect can be corrected (Destainville & Salomé 2006; Wong & Halvorsen 2006) it increases the error and should be avoided. We showed that with a gold nano-bead of 80 nm diameter, good results are achieved even at short exposure times as 1 ms.

2.1.4 Standard experimental set-up

Figure 3 (Nir, Lindner *et al.* 2011) shows a possible implementation of the experimental setup for TPM . It consists of a dark field (DF) microscope unit (Olympus BX-RLA2, Tokyo, Japan) with a x50 objective lens (NA=0.8) and an EM-CCD camera (Andor DU-885, Belfast, Northern Ireland) with a pixel size of 8x8 μm and a maximal pixel read-out rate of 35 MHz (Lindner, Nir *et al.* 2009).

The DF setup improves the signal to noise that is achieved in the measurement because it ensures that only the light that is scattered from the bead is collected by the objective lens, while eliminating the illumination background light.

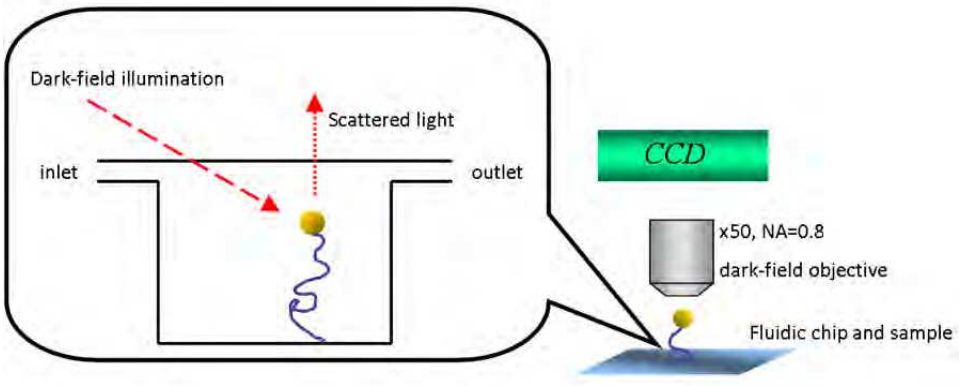

Fig. 3. The experimental setup. A dark-field microscope unit is used to track the metallic-bead position. A gold nano-bead is attached to DNA molecule and its position is tracked by the microscope and the CCD. When a protein interacts with the DNA, its biophysical properties are modified and can be tracked by the system.

2.1.5 Biochemical procedures

For constructing the dsDNA tethers it is common to use a PCR reaction to amplify desired dsDNA fragments from λ phage DNA. One end of the DNA is normally linked to digoxigenin (DIG) for a further attachment to an anti-DIG coated surface, this way the DNA is anchored to the surface. The other DNA end is biotin-linked for attaching a neutravidin conjugated nanobead. The modifications are done by using modified primers in the PCR reaction.

The tethering procedure is done in a flow cell and monitored with the microscope. First, a passivation procedure is required to reduce unspecific binding to the glass surface. Some common passivation reagents might be: Bio-Rad non-fat dry milk, Polyethylene Glycol (PEG) and Bovine Serum Albumin (BSA). After a proper incubation time (depends on the different passivation reagents) the buffer is washed and the surface is coated with anti-DIG. After one hour of incubation one should wash again and introduce the DNA to the solution. After incubation of one hour and another wash, the nano beads are introduced. After ~ 30 minutes of incubation and another wash the tethering procedure is complete (Selvin & Ha 2008; Lindner, Nir *et al.* 2009; Zimmermann, Nicolaus *et al.* 2010; Lindner, Nir *et al.* 2011).

2.1.6 Conducting experiments

First, each bead is measured a couple of times. The scattering plot is tested for circular symmetry. If it is found symmetric (figure 4), the persistence length is calculated (see section 2.1.6, data analysis). Measurement of the interaction of the bead with a protein continues only if its persistence length is ~50 ±5 nm. The next step would be to add an enzyme of interest, record the DNA's persistence length and realize if analyze the changes due to the enzyme acting on the DNA. Few beads are measured, few times each, in order to provide reliable statistic information. Each measurement consists of approximately ~2000 frames.

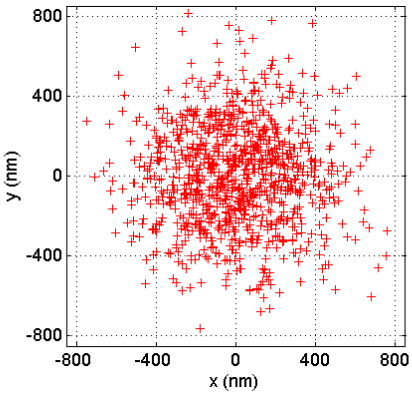

Fig. 4. *XY* projection. Each cross sign indicates a recording of the bead position at a time-point. Due to the symmetric polymer configurations distribution, the bead's distribution (representing the DNA end-to end vector) should be circular-symmetric centered at the DNA anchor point.

2.1.7 Data analysis

The data is analyzed with an SPT software package usually developed by the labs conducting such experiments with Matlab (The Mathworks, Natick, MA). For extraction of the DNA persistence length from the distribution, first, there should be an extraction of the bead position coordinates, $x(t), y(t)$ (2D projection) for each image (t). Then the radial distribution P(r) can be calculated and fitted to the expected distribution according to the Freely Joint Chain model which gives the Rayleigh distribution (Equation 6).

2.2 3D TPM

2.2.1 General description

3D TPM is an extended TPM method that was lately developed (Lindner, Nir *et al.* 2011). Instead of measuring only the 2D projection of the bead, it allows to measure the actual position of the bead in 3D.

The method relies on Total Internal Reflection (TIR), and employs the evanescent wave that is exponentially decreasing in the z-direction due to the TIR. Because the intensity depends on the bead height above the surface, the position of the bead in 3D can be determined.

2.2.2 Physical model

The intensity of an evanescent field decreases exponentially with the distance from the surface,

$$I = I_0 \exp(-z / d) \tag{8}$$

where I_0 is the intensity at the surface, z is the distance from surface, and d is the penetration depth. The penetration depth of the TIR illumination depends on a few fundamental parameter of the optical setup and can be tuned by changing the incident angle of the beam on the surface (Figure 5) according to:

$$d = \frac{\lambda_0}{4\pi\sqrt{n_i^2 \sin^2 \theta_i - n_t^2}} . \tag{9}$$

Here λ_0 is the wavelength of light in vacuum, n_i and n_t are the indexes of refraction of the materials above and below the surface and θ_i is the incident angle. By tuning the incident angle to be in the range of a few degrees above the critical angle, a penetration depth of 100–200 nm can be achieved, and axial distances in the range of 0–500 nm can be measured. Such a range is satisfying for measuring a 1-μm polymer with a persistence length of 50 nm; note that the end-to-end distance of such a polymer is rarely larger than 400 nm.

2.2.3 Standard experimental set-up

The experimental setup is very similar to a standard TPM setup, only with the addition of a diode laser and an equilateral prism to allow the creation of the evanescent wave (see figure 5).

2.2.4 Experimental procedures

A method that relies on the signal intensity to calculate the axial distance from the surface requires calibration in order to find d (Equation 9). We developed two calibration methods that rely on the actual system itself and do not require adding further optics to the setup. One is based on the 3D distribution of tethered beads (Volpe, Brettschneider *et al.* 2009). The distribution is measured with TIR illumination and the persistence length is calculated from the planar x and y distributions. Then, the distribution along z is fitted to the simulation results with a single parameter (the penetration depth d). The second method is based on

measuring the free diffusion of the beads. The principle is similar to the fluorescence correlation spectroscopy method described by Harlepp *et al.* (Harlepp, Robert *et al.* 2004).

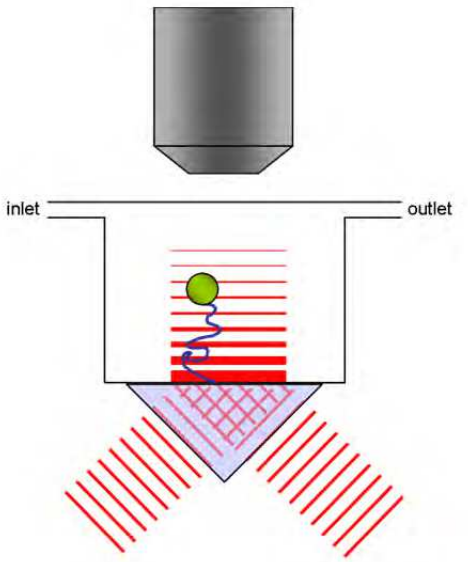

Fig. 5. 3D TPM illumination and detection. In order to achieve an evanescent wave, the light hits a prism above the critical angle. The evanescent wave decays exponentially into the sample while the bead's intensity and location is recorded. The bead position in along z is deduced according to Equation 8.

2.3 Single molecule force techniques

The following methods were thoroughly described before and hence will be briefly described here. Few key findings with these methods will be described as well.

So far we have only discussed a single molecule force-free technique. Although TPM allows us to observe a biopolymer in its natural form, it lacks the ability to manipulate the biopolymer. Many of the biological process such as DNA twisting, replication and cell migration are force driven. Another interesting fact is that biopolymers such as DNA, RNA, titin (the protein responsible for passive elasticity in the skeletal (Bustamante, Chemla *et al.* 2004)), etc posses "spring activity". If we combine these two facts, we can stretch and twist single biomolecules, hence examining their interactions with enzymes and regulating reaction coordinates as a function of load.

2.3.1 Magnetic tweezers

In magnetic tweezers a polymer of interest (such as DNA) is usually tethered to a glass surface while the other end is attached a magnetic microsphere which is pulled away from the surface with a magnet (Figure 6). The upper bound for force measurements in micromanipulation experiments is the tensile strength of a covalent bound, on the order of

1000 pN. The smallest measurable force is set by the Langevin force which is responsible for the Brownian motion of the sphere. Because of its random nature, the Langevin force is a noise density in force which is simply written as

$$f_n = \sqrt{4k_B T 6\pi\eta r} \tag{10}$$

where η is the viscosity of the medium and r is the radius of the particle. For a ~1 μm diameter microsphere in water, $f_n \sim 0.017\ pN/\sqrt{Hz}$. In between those two extremes lies the forces typical of the molecular scale, which is of order $k_B T / nm \sim 4pN$ (Strick, Allemand *et al.*). This is roughly the stall force of a single-molecular motor such as myosin (4 pN; (Finer, Simmons *et al.* 1994)) or RNA-polymerase (15–30 pN; (Yin, Landick *et al.* 1994; Wang 1998)). Applying forces in this regime on the magnetic microsphere, allows the delicate or aggressive stretching and twisting of the biopolymer, hence opening the door for manipulating single DNA-protein interactions (Manosas, Lionnet *et al.*; Bouchiat, Wang *et al.* 1999; Bustamante, Smith *et al.* 2000; Bustamante, Bryant *et al.* 2003; Neuman & Nagy 2008).

The most basic magnetic tweezers setup consists of a pair of permanent magnets, a flow cell, a magnetic bead and a CCD camera (Figure 6). For delicate manipulation, the magnet can be connected to a piezo-stage which allows bringing the magnets closer (for a stronger force) or away from the magnetic bead (for a weaker force) in nanometric steps.

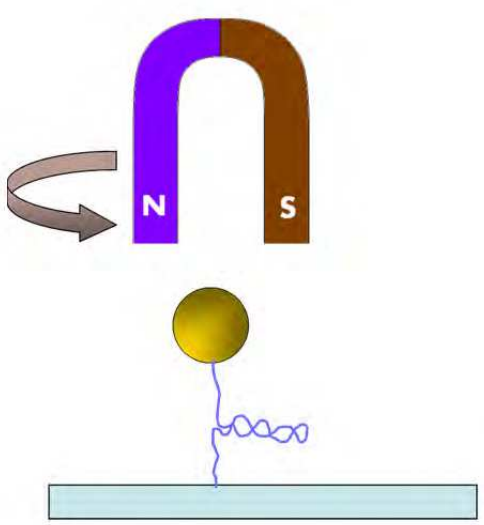

Fig. 6. Principle of magnetic tweezers. A magnetic force pulls the magnetic bead towards the magnet as a function of distance, stretching the DNA. The magnet can also be rotated, spinning the magnetic bead and twisting the DNA.

Figure 7 shows a typical plot that demonstrates how changing the force acting on the sphere allows the researchers to produce force-extension curves, meaning how much force is applied on the sphere to stretch a biopolymer to a certain extension.

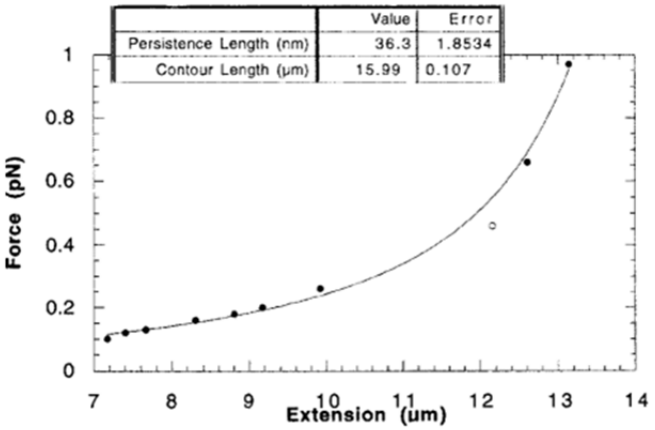

Fig. 7. Force-extension curve. Increasing the magnetic force results in further extension of the DNA. Reprinted with permission from (Haber & Wirtz 2000). Copyright [2000]. American Institute of Physics.

The Brownian fluctuations of the tethered sphere are equivalent to the motion of a damped pendulum of length $l =< z >$ (Strick, Allemand *et al.*). Pulling the bead along z direction gives rise to a magnetic force, F. Its longitudinal, δz^2 , and transverse fluctuations, δx^2 , can be characterized as a spring with an effective stiffness $k_z = \partial_z F$ and $k_x = F / l$. By the equipartition theorem they satisfy:

$$\delta z^2 = \frac{k_B T}{k_z} = \frac{k_B T}{\partial_z F} \tag{11a}$$

and

$$\delta x^2 = \frac{k_B T}{k_x} = \frac{k_B T l}{F} . \tag{11b}$$

Thus by tracking the sphere fluctuations it is possible to extract the force pulling the sphere (and the biopolymer).

2.3.2 Optical tweezers

The type of experiments usually done with optical tweezers are stretching experiments, where one stretches a biomolecules of interest, for example, DNA, and follows how these manipulations alter the DNA conformation or how do DNA binding proteins respond to the load applied on the DNA. It is also used to follow the changes in extension or force as a result of a biochemical process of the DNA with proteins. The optical tweezers are implemented by creating an optical trap which is implemented by concentrating a laser beam to a diffracted-limited spot through a high Numerical Aperture (NA) objective lens. When light hits a transparent dielectric object, such as a polystyrene microsphere, it has two

important optical outcomes (figure 8). The first one is reflection of the impinging light, which pushes away the microsphere (scattering force). The second one is refraction. The momentum of the light impinging on the microsphere is changed due to interaction with the microsphere. The momentum change of the light must be compensated by an equal and opposite change in momentum of the sphere, resulting in attraction of the sphere towards the center of the light spot (Williams 2002). To establish a stable trap, the force attracting the bead towards the light-spot must overcome the scattering force. The trap stiffness can be tuned by adjusting the laser intensity and focus. High NA objective lens is efficient at concentrating the light and stabilizes the trap. It is common to use high-power laser (>1 W) such as Nd:YAG and its derivatives that emit at the near-IR. The high-power reduces the spatial fluctuations of the trapped bead allowing a more stabilized trap and the near-IR wavelengths reduces the damage to the biomolecules that are in use (Neuman, Chadd *et al.* 1999). The detection of the microsphere is usually done with a quadrant photo-diode (QPD) which features high temporal resolution and leads to nanometric accuracy in detecting the deflection of the sphere (Rohrbach & AU - Stelzer 2002).

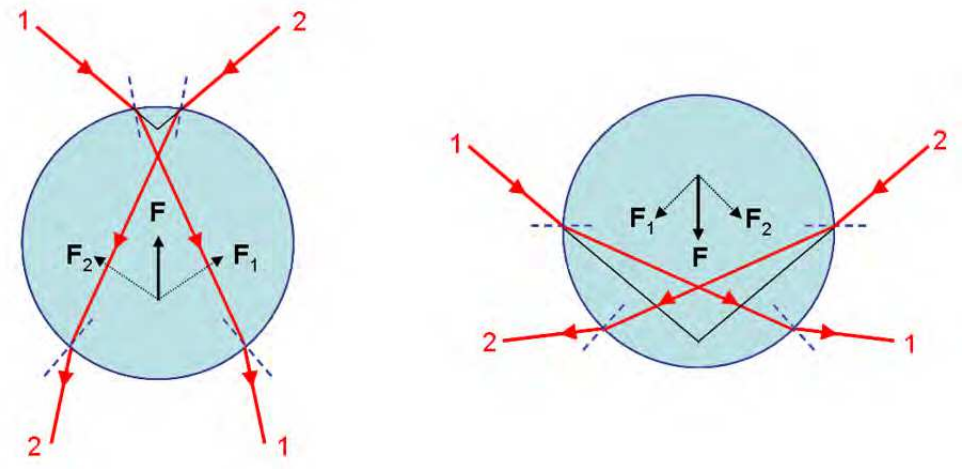

Fig. 8. Interaction of light with a transparent dielectric microsphere. Left: The microsphere is located beneath the center of the beam. When light hits the sphere it is reflected (not shown) and refracted according to Snell's law and the force acting on the object has to obey momentum conservation theory. Therefore, the net refraction force will point towards the center of the beam, pulling it up. Right: The microsphere is located above the center of the beam and the net refraction force is pointing towards the center of the beam, pulling it down.

An optical trap has to be calibrated for proper evaluating of the trap stiffness. The most common techniques treat the sphere as a linear spring, where the spring constant is determined by the sphere Brownian motion and the force obeys to Hooke's law ($f = -kx$). The sphere's position is calibrated by moving the sphere a known distance and recording

the signal at that position. It can also be tuned by analyzing the frequency response of the fluctuations (Bustamante, Macosko *et al.* 2000). More profound and detailed explanations can be found in (Neuman & Nagy 2008; Selvin & Ha 2008).

As was mentioned at the beginning of this section, the most common experiments with optical tweezers are stretching experiments, which produce force-extension curves. A dsDNA molecule in solution bends and curves locally according to thermal fluctuations, which is of course an entropic-driven behavior, influenced by the DNA elasticity. According to the Worm-like Chain (WLC) model that was briefly explained in section 2.1.2, the persistence length of a dsDNA in solution containing physiological salt conditions is 50 nm (Rubinstein & Colby 2003). The WLC model is well-suited to describe the entropic behavior of dsDNA in the regime of low and intermediate forces.

According to the model, the force F required to induce an extension x of the end-to-end distance of a polymer with a contour length L and persistence length l_p is given by: (Bustamante, Smith *et al.* 2000):

$$\frac{F \cdot l_p}{k_B T} = \frac{1}{4\left(1 - x/L\right)^2} + \frac{x}{L} - \frac{1}{4} \tag{12}$$

where k_B is the Boltzmann constant and T is the temperature.

2.3.3 Atomic force microscopy with tethered molecules

The Atomic Force Microscope (AFM) (Binnig, Quate *et al.* 1986; Martin, Williams *et al.* 1987) is another force-based technique that allows the stretching of individual biomolecules (Li, Wetzel *et al.* 2006; Perez-Jimenez, Garcia-Manyes *et al.* 2006; Neuman & Nagy 2008) and measure their elastic respond with sub-nanometer accuracy and picoNewton respond. Unlike previous-discussed single-molecule force spectroscopy methods, AFM is efficient also at high forces, which opened the door for exploring the properties of bio-entities in high-energy conformational states. For example, it enabled the detection of sub-Angstrom conformational changes of a single Dextran molecule (Walther, Bruji *et al.* 2006) and plot the unfolding force-histogram of a modular polyprotein (Li, Oberhauser *et al.* 2000).

In a typical experiment, a biomolecule of interest, say a protein, is linked to a flat surface that is mounted to on a piezoelectric stage. When the protein is approached by an AFM tip which is supported by a flexible cantilever, it might adsorb to the tip. When the tip is retreated from the surface it stretches the protein. The stretch bends the cantilever, which results in deflection of the laser beam impinging on the cantilever and recorded in a photo detector. If the cantilever elastic properties are known, it is possible to extract the force acting on the protein (Fisher, Oberhauser *et al.* 1999) (see figure 9). Low-force stretching can be modeled by the WLC model and the force acting on a polymer can be extracted in the same way done with optical tweezers according to equation 12. However, it was already mentioned that the great advantage in the AFM force spectroscopy technique is the ability to apply hundreds of picoNewtons . Moreover, force-extension curves for small or single-fold proteins are difficult to interpret because of non-specific interactions that might arise between the cantilever tip and the surface.

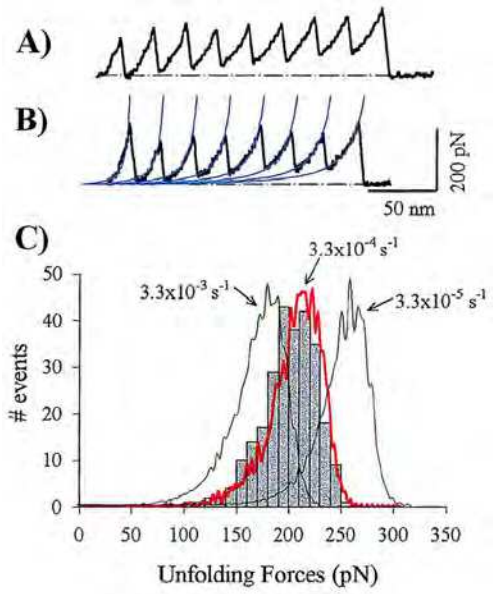

Fig. 9. Force–extension relationships for recombinant poly(I27) measured with AFM techniques. (A and B) Stretching of single I27GLG12 (A) or I27RS8 polyproteins (B) gives force–extension curves with a saw-tooth pattern having equally spaced force peaks. The saw-tooth pattern is well described by the WLC equation (continuous lines). (C) Unfolding force frequency histogram for I27RS8. The lines correspond to Monte Carlo simulations of the mean unfolding forces (n=10,000) of eight domains placed in series by using three different unfolding rate constants, k_u^0, an unfolding distance, Δx_u, of 0.25 nm, and a pulling rate of 0.6 nm/ms. Reprinted with permission from (Carrion-Vazquez, Oberhauser *et al*. 1999). PNAS.

To overcome this limitation and to utilize this technique advantages, modular proteins were engineered and formed "beads-on-a-string" structure (see figure 10). This structure is composed of tandem repeats of the same domain. At high forces (>100 pN), the domains are unfolded one-by-one, where each unfolding event is characterized by a saw-tooth in the force-extension curve and is explained as the elongation of the "string" due to the unfolding of a "bead" (domain) (Oberhauser, Marszalek *et al*. 1998). Each unfolding event can be fitted to the WLC model to recover the persistence length and the contour length of the polymer.

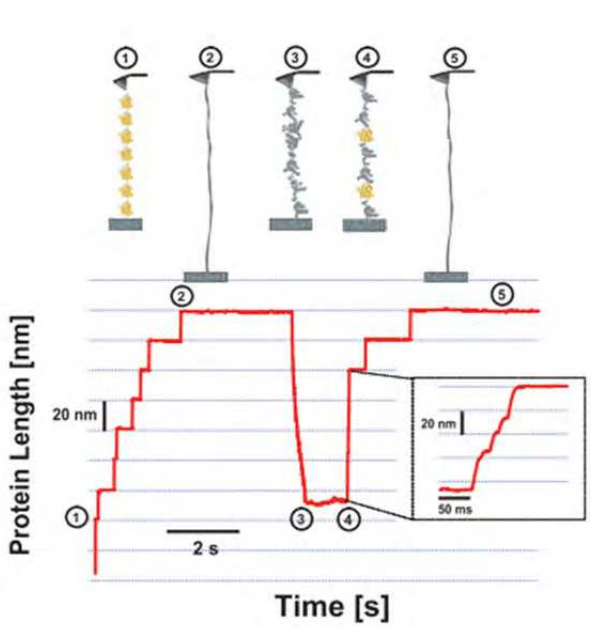

Fig. 10. 'Beads-on-a-string' stretching. At stage 1 the proteins are found at their native form (yellow). At stage 2 unfolding of the entire polyprotein occurs through pulling with the cantilever. For this protein (ubiquitin), it happens in 20 nm steps. At step 3 the force is quenched and the proteins maintain a collapsed form (gray). At step 4 refolding occur for some proteins along the chain and at step 5 the experiment is repeated by pulling again and causing another complete unfolding Reprinted with permission from (Garcia-Manyes, Dougan *et al.* 2009). PNAS.

2.4 Fluorescence resonance energy transfer with tethered molecules

Single-molecule FRET first introduced by Ha *et al.* (Ha, Enderle *et al.* 1996) is quite different from the other techniques discussed before. FRET aims to study the localization two entities in a biomolecule with a nanometer spatial resolution. This is done by measuring the non-radiative energy transfer from one fluorescent dye (donor) to another fluorescent dye (acceptor). The efficiency of energy transfer, E, depends on the donor-acceptor distance, R:

$$E = \frac{1}{1 + (R/R_0)^6} \tag{13}$$

Where R_0 is the distance when 50% of non-radiating energy transfer occurs (E=0.5) and is a function of the dyes properties (Selvin & Ha 2008). Due to the great sensitivity of this method to distance, it is applicable to a distance range of 3-8 nm. FRET is many times referred to as a spectroscopic ruler (figure 11). A biological molecule can be fluorescently-labeled in two sites, and intra-molecular dynamic motions of these sites relative to each other can be detected due to the energy transfer.

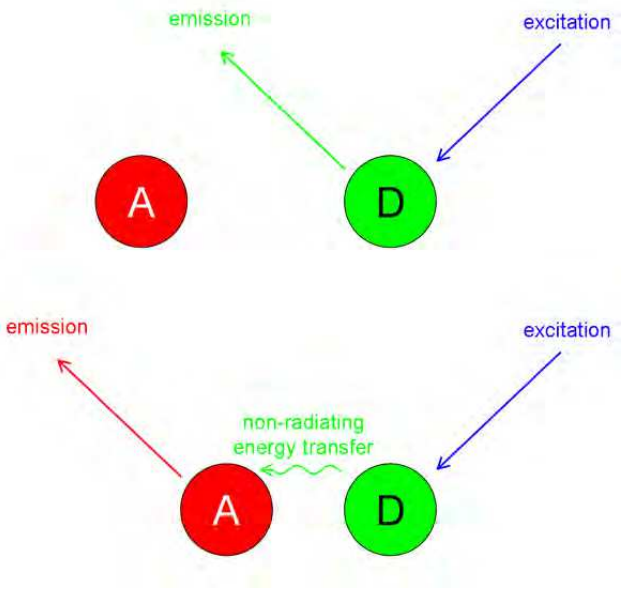

Fig. 11. FRET as a spectroscopic ruler. Up: The donor and acceptor dyes are too far for non-radiating energy transfer. Excitation of the donor results in its own emission. Down: The donor and acceptor are close enough for non-radiating energy transfer. Excitation of the donor might result in emission of the acceptor (other factors such as dipole-dipole orientation also affect the energy transfer).

Single molecule FRET (smFRET) has two major advantages over ensemble FRET. The first one derives from the fact that single-molecule experiments avoid averaging. smFRET allows the distinction between sub-populations and hence enables characterizing conformational states of biomolecules that result from dynamic and stochastic fluctuations. The second great advantage is the ability to observe in real-time dynamic events, an information that might be lost in ensemble FRET due to events being unsynchronized between different molecules.

In order to measure FRET, two detectors are needed, one for each dye. When there is a need for fast measurements and the signal is low, the preferred choice would be an Avalanche Photo-diode (APD), however choosing an Electron-Multiplying Charged Coupled Device (EMCCD) will enable visualizing hundreds of single-molecules simultaneously (Ha 2001). In smFRET the Signal-to-Noise Ratio (SNR) is relatively low (like most of the single-molecule experiments),so in order to decrease the auto fluorescence of the sample (noise) recorded by the detector, Total Internal Reflection Fluorescence microscopy (TIRF) is an appropriate solution. It ensures that only fluorescent dyes close to the surface are excited. smFRET can be applied to study surface-tethered dual-labeled DNA (McKinney, Declais *et al.* 2003) or the interactions between proteins and single tethered DNA (Myong, Rasnik *et al.* 2005; Myong, Bruno *et al.* 2007) or surface-tethered RNA (Arluison, Hohng *et al.* 2007).

3. Few key findings on relevant proteins

In this section we will show how the single molecule techniques that we described above, are employed to study a variety of biological processes such as: DNA bending by HU and IHF, DNA twisting by DNA gyrase, DNA replication by Φ29 DNA polymerase, refolding of ubiquitin and DNA unwinding by Hepatitis C virus NS3 helicase.

3.1 A DNA remodeling protein - HU

DNA-protein interactions are crucial also in bacteria cells where nucleoid-associated proteins (NAPs) together with macromolecular crowding effects play a major role in maintaining the architecture of the bacterial chromosome. NAPs ability to control the DNA structure is prominent for their role as regulators of DNA translocations (Krawiec & Riley 1990; Johnson, Johnson *et al.* 2005; Thanbichler, Wang *et al.* 2005; Luijsterburg, Noom *et al.* 2006; Stavans & Oppenheim 2006). Few of them were studied during the last decade with single molecule techniques and revealed new insights describing the dynamics of these protein-DNA/RNA interactions.

More than a few studies were performed on Integration Host Factor (IHF) protein of E. coli, which is involved in the integration of the bacteriophage λ DNA into the *E. coli* chromosome. In one of the studies, the local bending of a single 25 nm long DNA molecule caused by single IHF binding event was detected (Dixit, Singh-Zocchi *et al.* 2005). The experimental setup consisted of single linear dsDNA tethered at one end to a glass surface and to a microsphere at the other end. The tethered DNA had one consensus sequence for IHF binding. By optically monitoring the microsphere movement relative to the glass surface with evanescent microscopy, it was possible to detect conformational variations in the tether length. When IHF was introduced to the sample solution, the microsphere was pulled closer to the surface implying that the DNA bends and therefore adopts a more compact shape.

Another protein that belongs to the NAPs family is called Histone-like protein initially identified and characterized in *E.coli* strain U93 (HU). Ensemble studies revealed that the protein binds and bends DNA (Rouvière-Yaniv, Yaniv *et al.* 1979; Rouviere-Yaniv 1987; Pinson, Takahashi *et al.* 1999). Single molecule experiments refined this observation. They showed that while at relatively low HU concentrations the protein does compact the DNA, at high HU concentrations, it stretches the DNA (Sagi, Friedman *et al.* 2004; van Noort, Verbrugge *et al.* 2004; Skoko, Yoo *et al.* 2006; Xiao, Johnson *et al.* 2010). Some of these studies were performed with magnetic tweezers, (Figure 7) on a 50 nm dsDNA. Low concentrations of HU reduced the end-to-end distance in more than 50% but upon increasing the HU concentration, the persistence length increased up to ~150 nm. Similar results were also measured with a TPM setup (Figure 12). In comparison to the tweezers method, it has the advantage that force is not applied on the DNA and therefore the interaction occurs at the DNA natural form (Nir, Lindner *et al.* 2011). The bimodal effect of HU was recently explained by a model that assumes that the DNA is made of rigid segments and flexible joints (Rappaport & Rabin 2008). The model distinguishes two possible bending patterns along the polymer. If two neighboring segments are unoccupied by proteins, the bending angle θ is small, leading to the normal persistence length of DNA. When a protein occupies a segment without a neighboring protein, the spontaneous curvature increases, but when

proteins occupy both neighboring segments, the spontaneous curvature is reduced again. The model therefore predicts that the DNA contains bent joints (large spontaneous curvature) and unbent joints (small spontaneous curvature) along the same DNA strand. These findings contribute to our understanding that the DNA flexibility is a more localized term when DNA-bending proteins are involved. It also raises a discussion of the contradicting role of HU. It might be, that even a low HU concentration (could be just a few nM) is efficient for chromosome condensation while higher HU concentrations might provide a degree of freedom for the interplay of a more rigid form versus chromosome condensation during different cell phases.

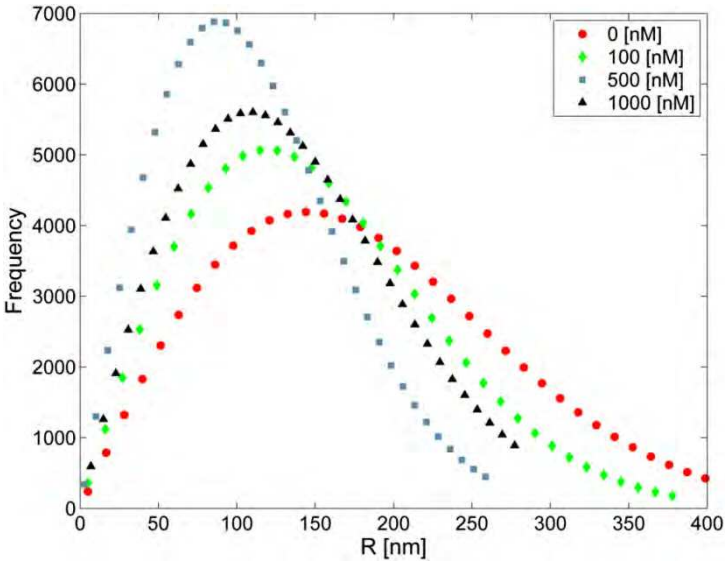

Fig. 12. Comparison of the radial distributions of the bead position for different HU concentrations as measured in a TPM experiment for the same bead. Circles represent DNA without HU proteins and the persistence length is 50 nm. Diamonds are for DNA in a solution with a concentration of 100 nM HU. The distribution is narrower compared to the HU-free DNA and the persistence length is ~39 nm. Squares represent DNA with HU concentration of 500 nM and the distribution is even narrower, with a persistence length of ~26 nm. Triangles represent DNA with HU concentration of 1000 nM and the distribution is now wider than for 500 nM with a persistence length of ~34 nm. Reprinted from Biophysical Journal **100** (2011) (Nir, Lindner *et al.* 2011) with permission from Elsevier.

So far we presented 2D TPM studies. Recently we expanded this method and made it possible to follow the DNA end-to-end distribution in 3D (Lindner, Nir *et al.* 2011). This study provided some powerful insights of the nature of the dynamic axial conformations (perpendicular to the surface) of tethered polymers. It was discovered that while the solution in the *XY* plane follows the normal distribution (Equation 5), the axial end-to-end distribution is different.

It can be described by a 1D random walk in half-space (Chandrasekhar 1943) and the solution is the difference between two Gaussians that centered around $\pm z_0$:

$$P(z)dz \propto \left[\exp\left(-\frac{3(z-z_0)^2}{4l_pL} \right) - \exp\left(-\frac{3(z+z_0)^2}{4l_pL} \right) \right] dz \tag{14}$$

where z_0 is some length parameter, between the width of a DNA (2nm) and its persistence length (50nm) , and it has a negligible effect on the solution. Using the 3D TPM, we measured this distribution, which is similar to the Rayleigh distribution.

Nevertheless, it is clear from the distribution that the DNA free end is repealed from surfaces. This effect may play an important role in experiments on DNA translocation through nanopores and nuclear pores, and should affect DNA dynamics in systems where it is tethered, such as the nucleus (where it is often attached to lamins).

3.2 Studying molecular motors with single molecule techniques

As mentioned above, single-molecule force-techniques enables one to study the mechanochemical properties of specific enzymes, and more specifically also the torque and twist of the DNA. Using these methods, an upgraded magnetic tweezers setup was built for studying the twist induced by *E. Coli* DNA gyrase in DNA (Gore, Bryant *et al.* 2006). Tension was generated in a single dsDNA by pulling a magnetic microsphere attached at one end of the tethered DNA, while a 'rotor' bead (Figure 13) is attached to the center of the DNA just below an engineered single strand nick, which acts as a free swivel. The angle of the rotor bead then reflects changes in twist of the lower DNA segment, and the angular velocity of the bead is proportional to the torque in this segment. Applying tension to the DNA causes changes in linking number to partition into DNA twist, resulting in a torque on the rotor bead. An enzymatic process that changes the linking number by two will cause the rotor bead to spin around twice as the DNA returns to its equilibrium conformation. Thus, the DNA construct serves as a self-regenerating substrate for DNA gyrase. Adding *E. Coli* DNA gyrase and 1 mM ATP results in bursts of directional rotation of the rotor bead, where each burst is an even number of rotations as predicted for type II Topoisomerase, when a single catalytic cycle changes the linking number by two (Brown & Cozzarelli 1979). In order to dissect the different mechanochemical steps of the supercoiling reaction, tension was applied in the range of 0.35-1.3 pN. It was found that the supercoiling velocity doesn't vary significantly, however the processivity and initiation rate have strong dependency to template tension. As the tension increased, bursts length decreased (processivity decreased) and waiting time between bursts increased (initiation rate decreased).

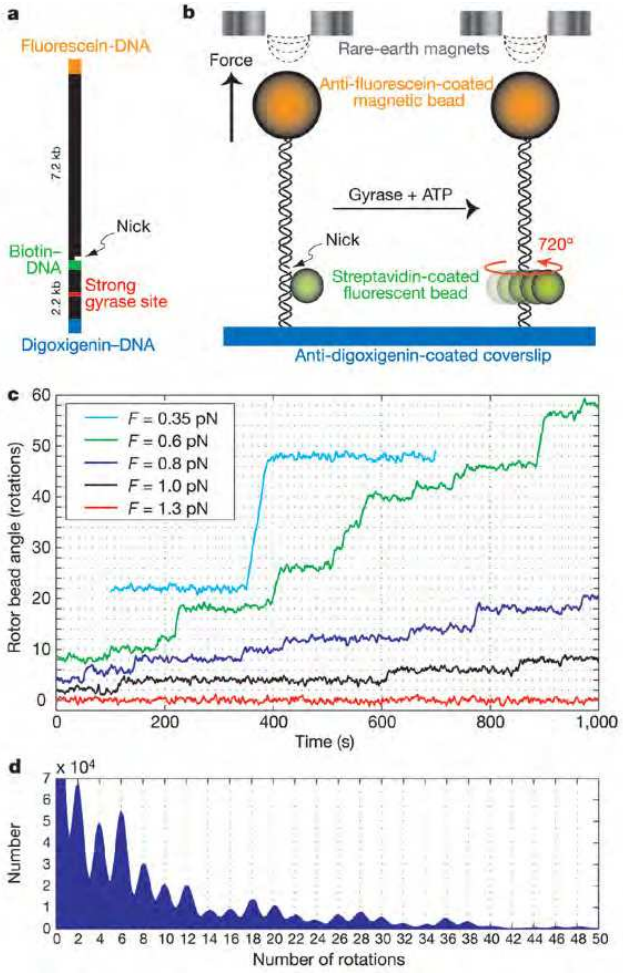

Fig. 13. Experimental design and single-molecule observations of gyrase activity. **a**, The molecular construct contains three distinct attachment sites and a site-specific nick, which acts as a swivel. A strong gyrase site was engineered into the lower DNA segment. **b**, Molecule and bead assemblies were constructed in parallel in a flow chamber and assayed by using an inverted microscope equipped with permanent magnets. Each molecule was stretched between the glass coverslip and a 1-μm magnetic bead, and a 530-nm diameter fluorescent rotor bead was attached to the central biotinylated patch. **c**, Plot of the rotor bead angle as a function of time (averaged over a 2-s window), showing bursts of activity due to diffusional encounters of individual gyrase enzymes. The activity of the enzyme is strongly dependent on tension. **d**, Histogram of the pairwise difference distribution function summed over 11 traces of 15–20 min (averaged over a 4-s window) at forces of 0.6–0.8 pN. The spacing of the peaks indicates that each catalytic cycle of the enzyme corresponds to two full rotations of the rotor bead, as expected for a type II topoisomerase such as DNA gyrase. Reprinted by permission from Macmillan Publishers Ltd: [Nature](Gore, Bryant *et al.* 2006), copyright (2006).

The measured data indicating of untwisting events caused by single DNA gyrase, allowed the researchers to build a physical model for the gyrase-DNA complex kinetics. Such a model cannot be deduced unless the single-molecule data is known.

3.3 DNA replication studies

Another study exploited the ability to apply tension on single DNA tethers using optical tweezers to investigate the conformational dynamics of the intramolecular DNA primer transfer during the processive replicative activity of the Φ29 DNA polymerase and two of its mutants (Ibarra, Chemla *et al.* 2009). Φ29 DNA polymerase has a catalytic unit as well as an exonuclease unit, allowing it to replicate DNA and fix base-pair mismatching at the same time.

The authors used optical tweezers to apply mechanical tension between two beads attached to the ends of an 8-kb dsDNA molecule with a ~400 nucleotide single-stranded gap in the middle (Figure 14A). They monitored the change in the end-to-end distance of the DNA (Δx) at constant force as the single-stranded template is replicated to dsDNA by Φ29 DNA polymerase (Figure 14B). The number of nucleotides incorporated as a function of time was obtained by dividing the observed distance change (Δx) by the expected change at a given force accompanying the conversion of one single-stranded nucleotide into its double-stranded counterpart. They also detected pause events as shown in Figure 14C.

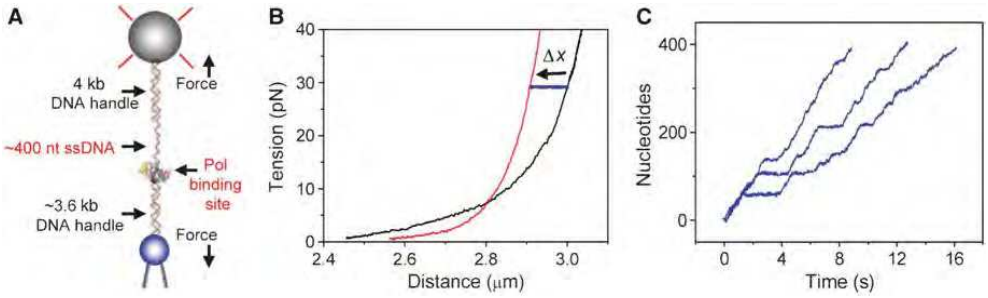

Fig. 14. Experimental set-up and detection of single-molecule polymerization events.
(A) Schematic representation of the experimental set-up (not to scale). A single DNA molecule was tethered to functionalized beads using biotin and digoxigenin moieties at the distal ends of the molecule. One bead (blue) is held in place at the end of a micropipette and the other (grey) by the optical trap. **(B)** Replication experiment (29±0.8 pN, wt polymerase) showing the force-extension curves of the initial (black) and final (red) DNA molecules. At constant force, replication shortens the distance (Δx , blue) between the beads.
(C) Representative replication traces from three independent experiments (22±0.8 pN, ed mutant). Reprinted by permission from Macmillan Publishers Ltd: [EMBO J] (Ibarra, Chemla *et al.* 2009),copyright (2009).

The authors observed an initial sharp increase in the relative pause occupancy and rationalized that it indicates that access to this intermediate from the initial pol1 (initial pol cycle) is force-sensitive and the ensuing saturation requires that the equilibrium between the intermediate and the paused state, Kp, be insensitive to the template tension. Importantly,

this new intermediate must be a moving or polymerization-competent cycle (that the authors call pol2), as direct access to a non-active state in a tension-sensitive manner would lead to a continuous exponential increase in the relative pause occupancy, which was not observed.

3.4 Protein refolding studies

Understanding the dynamics of protein folding and unfolding is an ongoing effort that is presumed to benefit a lot from force spectroscopy. Single-molecule force spectroscopy techniques allow the detailed examination of the free-energy surface over which a protein diffuses in response to a mechanical perturbation (Schuler, Lipman *et al.* 2002; Rhoades, Gussakovsky *et al.* 2003). It is possible to pull a protein with an AFM tip and unfold it, a reversible process according to (Rief, Gautel *et al.* 1997; Carrion-Vazquez, Oberhauser *et al.* 1999) and upon reducing the pulling force, the unfolded protein begins to fold from a highly extended conformation that is rare or nonexistent in solution, even in the presence of denaturants. For example, at a typical force of 110 pN, mechanically unfolded ubiquitin proteins extend by >80% of their contour length (~20 nm) (Schlierf, Li *et al.* 2004). By contrast, ubiquitin proteins unfolded chemically in solution by 6 M guanidinium chloride stay compact, with a radius of gyration of only ~2.6 nm (Jacob, Krantz *et al.* 2004; Kohn, Millett *et al.* 2004).

Garcia-Manyes *et al.* studied the collapse and re-folding trajectories of ubiquitin polyproteins (Garcia-Manyes, Bruji *et al.* 2007). A chain of ubiquitin polyproteins was engineered and adsorbed to a surface while its other end was pulled by a force of 110 pN to unfold the polyproteins chain (Garcia-Manyes, Dougan *et al.* 2009). Unfolding events were observed as 20 nm steps (for each protein unfolding), followed by force-quenching to 10 pN. The time spent at the quenched state, Δt, was changed between 0.2-15 seconds before pulling again. The quenching leads to collapsed state which is mechanically unstable that is followed by folding of the protein to the native state. Therefore, changing the duration of the quenched state allows to probe the folding duration. For short durations (Δt =100-200 ms), the unfolding trajectory unravels rapidly and the 20 nm stepwise mechanism is not observed. It indicates that the proteins were not able to fold to their native state. Increasing Δt to 500 ms leads to the detection of steps when re-applying force and they predominant at Δt =3 seconds (Figure 15A). In figure 15B, a two-state process is observed, a fast initial extension that unravels the collapsed states in a stepwise manner featuring different lengths and followed by a much slower staircase of 20-nm steps, characteristic of fully refolded ubiquitin. The two states can be described by a bi-exponential fit with two rate constants, k_1 for the fast stage and k_2 for the slow state, both showing no dependency in Δt, suggesting that the protein does not gradually progress from higher to lower energy states, but populates two distinct conformational states.

The authors adopted the two-state model stating that the fast phase is a mechanically-weak state composed of a number of possible conformations with an equal distance from the transition state corresponding to the unfolding of the native state. With that knowledge, the authors tried to address the question whether these structures represent necessary folding precursors or unproductive kinetic traps in the folding energy landscape. They therefore devised a protocol to disrupt these collapsed conformations by interrupting the folding trajectories with a brief (100 ms) pulse to a higher force of 60 pN. During such a brief pulse,

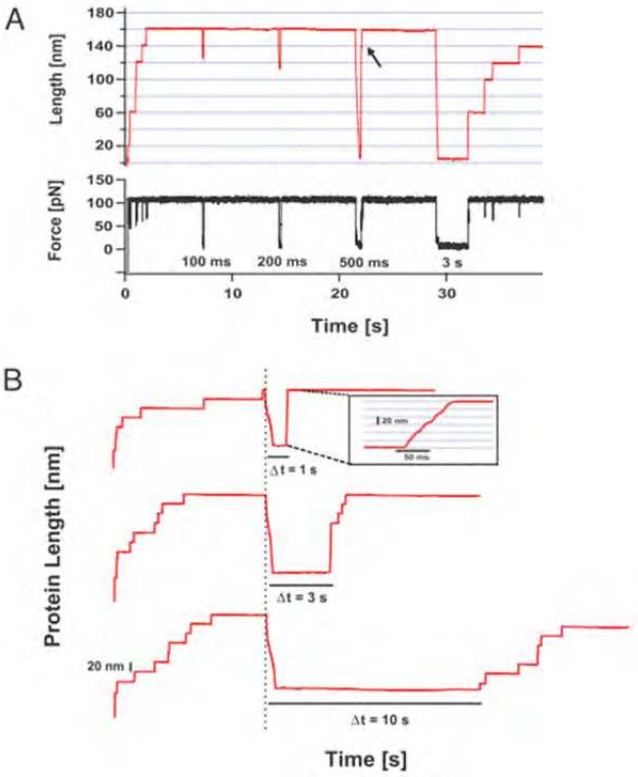

Fig. 15. Identification of a weakly stable ensemble of collapsed conformations in the folding of ubiquitin. **(A)** The authors repeatedly unfold and extend a ubiquitin polyprotein at 110 pN and then reduce the force to 10 pN for a varying amount of time, Δt, to trigger folding. First the polyprotein elongates in well defined steps of 20 nm, because each protein in the chain unfolds at a high force. Upon quenching the force the extended protein collapses. The state of the collapsed polypeptide was probed by raising the force back to 110 pN and measuring the kinetics of the protein elongation. **(B)** After full collapse the protein becomes segregated into 2 distinct ensembles: The first is identified by a fast heterogeneous elongation made of multiple sized steps (Inset); the second corresponds to well defined steps of 20 nm that identify fully folded proteins. The ratio between these 2 states of the protein depends on Δt and longer values of Δt favor the native ensemble. (Garcia-Manyes, Dougan *et al.* 2009). Reprinted with permission of PNAS.

native ubiquitin has a very low probability of unfolding. If the set of mechanically-unstable collapsed conformations are a prerequisite to folding, their disruption would cause a delay in the recovery of mechanical stability as compared with the unperturbed trajectories. By contrast, if the collapsed states represent unproductive traps, then unraveling them would accelerate the rate of folding. The authors showed that an average unfolding trajectory after 5 s of folding has a higher content of folded proteins than the same trajectory with the mechanical interruption. They concluded that the collapsed conformations are necessary precursors of the folded state.

3.5 Studying the unwinding of DNA by hepatitis C virus NS3 helicase

In this final example, the unwinding of DNA is demonstrated by using smFRET. In hepatitis C virus (HCV), nonstructural protein 3 (NS3) is an essential component of the viral replication complex that works with the polymerase NS5B and other protein cofactors (such as NS4A, NS5A, and NS2) to ensure effective copying of the virus. Myong *et al.* used single-molecule FRET to resolve the individual steps of DNA unwinding, catalyzed by NS3 in the absence of applied force (Myong, Bruno *et al.* 2007). Two DNA substrates were prepared. Both consisted of 18 bp and a 3'-ssDNA tail (20 nt) to create a double stranded – single stranded junction as an anchoring position to the helicase and the DNA tail was anchored to the surface. One DNA fragment had a donor and an acceptor fluorophores (cy3 and cy5 respectively) attached to the two different DNA strands at the junction through aminodeoxythymidine (figure 16A). The other DNA fragment had the dyes attached 9 bp away from the junction so that FRET signal is sensitive only to the final 9-bp unwinding

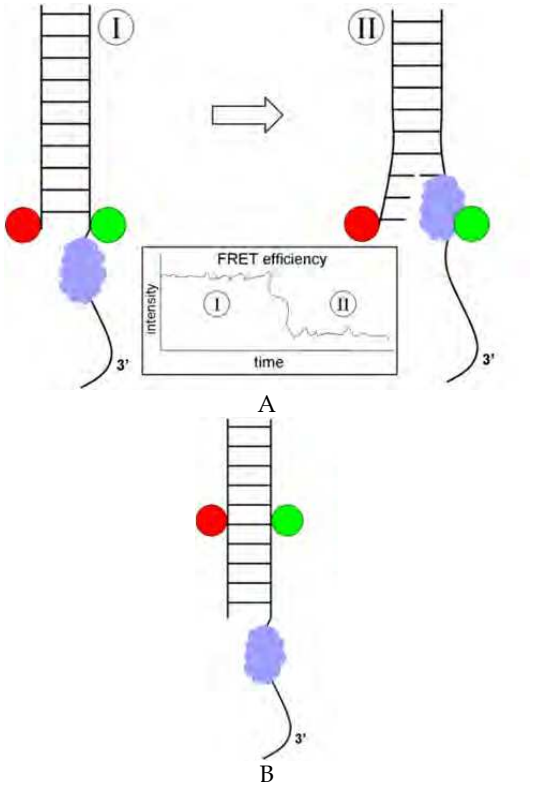

Fig. 16. DNA template for smFRET. **(A)** NS3 helicase translocates on a single dsDNA with a ssDNA tail. A green donor and a red acceptor dyes are attached at the end of the dsDNA template. At state I, the two dyes are close and the FRET efficiency (inset) is high. At state II, the initially dsDNA is partially unwound increasing the distance between the two dyes and resulting in low FRET efficiency. **(B)** In this setup the dyes are attached to the DNA in the middle of the dsDNA.

(figure 16B). Addition of ATP resulted in a decrease of the FRET efficiency as a result of strand separation due to the helicase unwinding. 6 and 3 steps were detected for the 18 bp dsDNA and 9 bp dsDNA respectively, indicating of strand separation in 3 bp steps. If hydrolysis of a single ATP results in a 3-bp step than the dwell time histogram of the steps would follow a single-exponential decay. However the observation revealed non-exponential dwell time histograms.

The authors derived a model suggesting that domains I&II of the helicase move forward one bp at a time and at the third step, the spring-loaded domain 3 moves forward in a burst motion, unzipping 3 bp as a consequence.

4. Conclusions

Single-molecule techniques are an essential tool that opened the door for high temporal and spatial studies, providing the ability to manipulate or passively observe single molecules. We presented some of the major single molecules methods and few applications of these methods for studying key biochemical processes such as DNA replication, protein folding and DNA remodeling. Table 1 summarizes the methods presented here and compares them.

	TPM	**Magnetic Tweezers**	**Optical Tweezers**	**AFM**	**smFRET**
Relies on	Probe's Brownian motion	Application of magnetic force	Momentum change of incident light	Stretching a single molecule with an AFM cantilever	Resonant Energy transfer
Probe	Nanometric gold bead	Polystyrene microsphere	Polystyrene microsphere	Cantilever	Fluorescent dyes
Range of forces (pN)	0	10^{-3} - 10^{2}	10^{-1} - 10^{2}	10 - 10^{4}	0
Data produced	Scattering plot (Fig.4)	Force-extension curve (Fig.7)	Force-extension curve (Fig. 14b)	Force-extension curve (Fig.16)	Energy transfer efficiency

Table 1. A comparison of single-molecule techniques reviewed here.

TPM and smFRET allows to measure without applying force and hence are good candidates to describe DNA-protein interactions in their native forms. On the other hand, force-based techniques allows to manipulate single-molecules and enable to study these interactions in extreme conditions, introducing higher energy states that are usually not observed. They reveal the mechanochemical properties of single enzymes. We showed that using TPM we were able to observe end-to-end fluctuations of single DNA molecules and measure their persistence length dynamic variations induced by HU protein. We proved that the bimodal effect of HU exists even without the use of force.

We showed how magnetic tweezers can be implemented to study the probability of DNA gyrase to achieve a productive catalytic cycle. Optical tweezers were demonstrated as a tool for discovering the proofreading activity of DNA polymerase, revealing the different steps comprising the transition from polymerase activity to exonuclease activity within the same enzyme. The use of AFM was demonstrated for catalyzing the unfolding of single proteins and then the refolding dynamics leading to the collapsed followed by the native state. Finally, smFRET was reviewed for studying helicase motor enzyme mechanisms.

All together these techniques span a broad spectrum of capabilities that can unravel different properties of single DNA-protein interactions and provide unprecedented details that are not visible by ensemble techniques. These properties includes rate constants measured directly on a single molecule, motor enzymes mechanisms, elastic and chemical properties of single molecules and high-energy states.

5. Near-future capabilities

The methodology of single molecule techniques is rapidly growing. Although the achievements that were demonstrated here, and many others, indicate on the usefulness of the existing methods, there are still important challenges that call for further improvements. High spatial resolution and high temporal resolution are necessary, especially with optical methods that can be applied to single molecules. These may be achieved with the newly developed super-resolution techniques such as stimulated depletion emission (STED), 4-pi microscopy, Photoactivated localization microscopy (PALM), stochastic optical reconstruction microscopy (STORM) and others.

Another promising direction relies on nano-optics. Due to improvements in lithography methods, it is now possible to design and fabricate nano-sized devices such as metal-based structures that use plasmonic effects. It was already shown that plasmonic nano-antennas are capable of concentrating an intense light to a sub-diffracted volume (Grigorenko, Roberts *et al.* 2008; Righini, Volpe *et al.* 2008; Huang, Maerkl *et al.* 2009; Juan, Righini *et al.* 2011) and trap dielectric particles and even *E. Coli* bacteria. These plasmonic traps do not require bulk optics (such as optical tweezers) and restrict the trapped object to a smaller volume.

Another intriguing capability is the emerging of different illumination techniques. For instance, the ability to manipulate single molecules under white light and observe fluorescent-conjugated enzymes translocating on single DNAs is fascinating and provide us with further information of the reactions nature since it enables us to follow the dynamics of both a trapped biomolecule and an enzyme translocating on it. One example is the "fleezers", fluorescent tweezers (Comstock, Ha *et al.* 2011). In this setup a dual optical trap integrated with a confocal microscope to illuminate fluorescent molecules was implemented to observe individual single fluorophore–labeled DNA oligonucleotides binding and unbinding to a complementary DNA suspended between two trapped beads.

We will finish by mentioning solid-state nanopores. Nanometer-sized holes in a thin synthetic membrane are a versatile tool for the detection and manipulation of charged biomolecules. For example, a single DNA molecule that translocates through the nanopore

will have a unique signature that is attributed to its sequence. That can be done by applying an external electric field which drives a biomolecule through the nanopore, producing a characteristic transient change in the trans-pore ionic current (Heng, Ho *et al.* 2004; Garaj, Hubbard *et al.* 2010; Stefan, Alexander *et al.* 2011).

6. Acknowledgements

This work was supported in part by the Israel Science Foundation grants 985/08, 1729/08, 1793/07, and 25/07.

7. References

Arluison, V., S. Hohng, R. Roy, O. Pellegrini, P. Regnier & T. Ha (2007). Spectroscopic Observation of RNA Chaperone Activities of Hfq in Post-Transcriptional Regulation by a Small Non-Coding RNA. *Nucl. Acids Res*, 353, pp. 999-1006

Binnig, G., C. F. Quate & C. Gerber (1986). Atomic Force Microscope. *Phys. Rev. Lett*, 569, pp. 930

Bouchiat, C., M. D. Wang, J.-F. Allemand, T. Strick, S. M. Block & V. Croquette (1999). Estimating the Persistence Length of a Worm-Like Chain Molecule from Force-Extension Measurements. *Biophys. J*, 76, pp. 409-413

Brown, P. O. & N. R. Cozzarelli (1979). A Sign Inversion Mechanism for Enzymatic Supercoiling of DNA. *Science*, 2064422, pp. 1081-1083

Bustamante, C., Z. Bryant & S. B. Smith (2003). Ten Years of Tension: Single-Molecule DNA Mechanics. *Nature*, 4216921, pp. 423-427

Bustamante, C., Y. R. Chemla, N. R. Forde & D. Izhaky (2004). Mechanical Processes in Biochemistry. *Annu. Rev. Biochem*, 731, pp. 705-748

Bustamante, C., J. C. Macosko & G. J. L. Wuite (2000). Grabbing the Cat by the Tail: Manipulating Molecules One by One. *Nat. Rev. Mol. Cell Biol*, 1, pp. 131-136

Bustamante, C., S. B. Smith, J. Liphardt & D. Smith (2000). Single-Molecule Studies of DNA Mechanics. *Curr. Opin. Struct. Biol*, 103, pp. 279-285

Carrion-Vazquez, M., A. F. Oberhauser, S. B. Fowler, P. E. Marszalek, S. E. Broedel, J. Clarke & J. M. Fernandez (1999). Mechanical and Chemical Unfolding of a Single Protein: A Comparison. *Proc. Natl. Acad. Sci. U S A*, 967, pp. 3694-3699

Chandrasekhar, S. (1943). Stochastic Problems in Physics and Astronomy. *Rev. Mod. Phys*, 151, pp. 1

Comstock, M. J., T. Ha & Y. R. Chemla (2011). Ultrahigh-Resolution Optical Trap with Single-Fluorophore Sensitivity. *Nat. Meth*, 84, pp. 335-340

Destainville, N. & L. Salomé (2006). Quantification and Correction of Systematic Errors Due to Detector Time-Averaging in Single-Molecule Tracking Experiments *Biophys. J*, 902, pp. L17-L19

Dixit, S., M. Singh-Zocchi, J. Hanne & G. Zocchi (2005). Mechanics of Binding of a Single Integration-Host-Factor Protein to DNA. *Phys. Rev. Lett*, 9411, pp. 118101

Finer, J. T., R. M. Simmons & J. A. Spudich (1994). Single Myosin Molecule Mechanics: Piconewton Forces and Nanometre Steps. *Nature*, 3686467, pp. 113-119

Fisher, T. E., A. F. Oberhauser, M. Carrion-Vazquez, P. E. Marszalek & J. M. Fernandez (1999). The Study of Protein Mechanics with the Atomic Force Microscope. *Trends Biochem. Sci*, 2410, pp. 379-384

Garaj, S., W. Hubbard, A. Reina, J. Kong, D. Branton & J. A. Golovchenko (2010). Graphene as a Subnanometre Trans-Electrode Membrane. *Nature*, 4677312, pp. 190-193

Garcia-Manyes, S., Bruji, cacute, Jasna, C. L. Badilla & J. M. Fernandez (2007). Force-Clamp Spectroscopy of Single-Protein Monomers Reveals the Individual Unfolding and Folding Pathways of I27 and Ubiquitin. *Biophys. J*, 937, pp. 2436-2446

Garcia-Manyes, S., L. Dougan, C. L. Badilla, J. Bruji & J. M. Fernandez (2009). Direct Observation of an Ensemble of Stable Collapsed States in the Mechanical Folding of Ubiquitin. *Proc. Natl. Acad. Sci. U S A*,

Gore, J., Z. Bryant, M. D. Stone, M. Nollmann, N. R. Cozzarelli & C. Bustamante (2006). Mechanochemical Analysis of DNA Gyrase Using Rotor Bead Tracking. *Nature*, 4397072, pp. 100-104

Grigorenko, A. N., N. W. Roberts, M. R. Dickinson & Y. Zhang (2008). Nanometric Optical Tweezers Based on Nanostructured Substrates. *Nat. Photon*, 26, pp. 365-370

Ha, T. (2001). Single-Molecule Fluorescence Resonance Energy Transfer. *Methods*, 25, pp. 78-86

Ha, T., T. Enderle, D. F. Ogletree, D. S. Chemla, P. R. Selvin & S. Weiss (1996). Probing the Interaction between Two Single Molecules: Fluorescence Resonance Energy Transfer between a Single Donor and a Single Acceptor. *Proc. Natl. Acad. Sci. U S A*, 93, pp. 6264–6268

Haber, C. & D. Wirtz (2000). Magnetic Tweezers for DNA Micromanipulation. *Rev. Sci. Instrum.*, 7112, pp. 4561

Harlepp, S., J. Robert, N. C. Darnton & D. Chatenay (2004). Subnanometric Measurements of Evanescent Wave Penetration Depth Using Total Internal Reflection Microscopy Combined with Fluorescent Correlation Spectroscopy. *Applied Physcis Letters*, 85, pp. 3917-3919

Heng, J. B., C. Ho, T. Kim, R. Timp, A. Aksimentiev, Y. V. Grinkova, S. Sligar, K. Schulten & G. Timp (2004). Sizing DNA Using a Nanometer-Diameter Pore. *Biophys. J*, 874, pp. 2905-2911

Huang, L., S. J. Maerkl & O. J. Martin (2009). Integration of Plasmonic Trapping in a Microfluidic Environment. *Opt. Express*, 178, pp. 6018-6024

Ibarra, B., Y. R. Chemla, S. Plyasunov, S. B. Smith, J. M. Lazaro, M. Salas & C. Bustamante (2009). Proofreading Dynamics of a Processive DNA Polymerase. *EMBO J*, 2818, pp. 2794-2802

Jacob, J., B. Krantz, R. S. Dothager, P. Thiyagarajan & T. R. Sosnick (2004). Early Collapse Is Not an Obligate Step in Protein Folding. *J. Mol. Biol*, 3382, pp. 369-382

Jeon, J.-H. & R. Metzler (2010). Fractional Brownian Motion and Motion Governed by the Fractional Langevin Equation in Confined Geometries. *Phys. Rev. E*, 812, pp. 021103

Johnson, R. C., L. M. Johnson, J. W. Schmidt & J. F. Garder (2005). Major Nucleoid Proteins in the Structure and Function of the *Escherichia Coli* Chromosome. In: *The Bacterial Chromosome*. N. P. Higgins. 1**:** 65-132, American Society for Microbiology. Washington, DC.

Juan, M. L., M. Righini & R. Quidant (2011). Plasmon Nano-Optical Tweezers. *Nat. Photon*, 56, pp. 349-356

Kohn, J. E., I. S. Millett, *et al.* (2004). Random-Coil Behavior and the Dimensions of Chemically Unfolded Proteins. *Proc. Natl. Acad. Sci. U S A*, 10134, pp. 12491-12496

Krawiec, S. & M. Riley (1990). Organization of the Bacterial Chromosome. *Microbiol. Rev.*, 544, pp. 502-539

Li, H., A. F. Oberhauser, S. B. Fowler, J. Clarke & J. M. Fernandez (2000). Atomic Force Microscopy Reveals the Mechanical Design of a Modular Protein. *Proc. Natl. Acad. Sci. U S A*, 9712, pp. 6527-6531

Li, L., S. Wetzel, A. Pluckthun & J. M. Fernandez (2006). Stepwise Unfolding of Ankyrin Repeats in a Single Protein Revealed by Atomic Force Microscopy. *Biophys. J*, 904, pp. L30-L32

Lindner, M., G. Nir, H. R. C. Dietrich, Ian T. Young, E. Tauber, I. Bronshtein, L. Altman & Y. Garini (2009). Studies of Single Molecules in Their Natural Form. *Isr. J. Chem*, 493-4, pp. 283-291

Lindner, M., G. Nir, S. Medalion, H. R. C. Dietrich, Y. Rabin & Y. Garini (2011). Force-Free Measurements of the Conformations of DNA Molecules Tethered to a Wall. *Phys. Rev. E*, 831, pp. 011916

Luijsterburg, M. S., M. C. Noom, G. J. L. Wuite & R. T. Dame (2006). The Architectural Role of Nucleoid-Associated Proteins in the Organization of Bacterial Chromatin: A Molecular Perspective. *J. Struct. Biol*, 1562, pp. 262-272

Manosas, M., T. Lionnet, E. Praly, D. Fangyuan, J.-F. Allemand, D. Bensimon, V. Croquette & V. Rivasseau Studies of DNA-Replication at the Single Molecule Level Using Magnetic Tweezers. *Biological Physics*, 60, pp. 89-122

Martin, Y., C. C. Williams & H. K. Wickramasinghe (1987). Atomic Force Microscope - Force Mapping and Profiling on a Sub 100 Å Scale. *J. Appl. Phys*, 6110, pp. 4723-4729

McKinney, S. A., A.-C. Declais, D. M. J. Lilley & T. Ha (2003). Structural Dynamics of Individual Holliday Junctions. *Nat. Struct. Mol. Biol*, 102, pp. 93-97

Myong, S., M. M. Bruno, A. M. Pyle & T. Ha (2007). Spring-Loaded Mechanism of DNA Unwinding by Hepatitis C Virus Ns3 Helicase. *Science*, 3175837, pp. 513-516

Myong, S., I. Rasnik, C. Joo, T. M. Lohman & T. Ha (2005). Repetitive Shuttling of a Motor Protein on DNA. *Nature*, 4377063, pp. 1321-1325

Nelson, P. C., C. Zurla, D. Brogioli, J. F. Beausang, L. Finzi & D. Dunlap (2006). Tethered Particle Motion as a Diagnostic of DNA Tether Length. *J. Phys. Chem. B*, 11034, pp. 17260-17267

Neuman, K. C., E. H. Chadd, G. F. Liou, K. Bergman & S. M. Block (1999). Characterization of Photodamage to Escherichia Coli in Optical Traps. *Biophys. J*, 775, pp. 2856-2863

Neuman, K. C. & A. Nagy (2008). Single-Molecule Force Spectroscopy: Optical Tweezers, Magnetic Tweezers and Atomic Force Microscopy. *Nat. Meth*, 56, pp. 491-505

Nir, G., M. Lindner, H. R. C. Dietrich, O. Girshevitz, C. E. Vorgias & Y. Garini (2011). HU Protein Induces Incoherent DNA Persistence Length. *Biophys. J*, 100, pp. 784-90

Oberhauser, A. F., P. E. Marszalek, H. P. Erickson & J. M. Fernandez (1998). The Molecular Elasticity of the Extracellular Matrix Protein Tenascin. *Nature*, 3936681, pp. 181-185

Perez-Jimenez, R., S. Garcia-Manyes, S. R. K. Ainavarapu & J. M. Fernandez (2006). Mechanical Unfolding Pathways of the Enhanced Yellow Fluorescent Protein Revealed by Single Molecule Force Spectroscopy. *J. Biol. Chem*, 28152, pp. 40010-40014

Pinson, V., M. Takahashi & J. Rouviere-Yaniv (1999). Differential Binding of the *Escherichia Coli* HU, Homodimeric Forms and Heterodimeric Form to Linear, Gapped and Cruciform DNA. *J. Mol. Biol*, 287, pp. 485-497

Rappaport, S. M. & Y. Rabin (2008). Model of DNA Bending by Cooperative Binding of Proteins. *Phys. Rev. Lett*, 1013, pp. 038101

Rhoades, E., E. Gussakovsky & G. Haran (2003). Watching Proteins Fold One Molecule at a Time. *Proc. Natl. Acad. Sci. U S A*, 1006, pp. 3197-3202

Rief, M., M. Gautel, F. Oesterhelt, J. M. Fernandez & H. E. Gaub (1997). Reversible Unfolding of Individual Titin Immunoglobulin Domains by AFM. *Science*, 2765315, pp. 1109-1112

Righini, M., G. Volpe, C. Girard, P. Dimitri & R. Quidant (2008). Surface Plasmon Optical Tweezers: Tunable Optical Manipulation in the Femtonewton Range. *Phys. Rev. Lett*, 10018, pp. 186804

Rohrbach, A. & E. AU - Stelzer (2002). Three-Dimensional Position Detection of Optically Trapped Dielectric Particles. *J. Appl. Phys.*, 918,

Rouvière-Yaniv, J., M. Yaniv & J.-E. Germond (1979). E. Coli DNA Binding Protein HU Forms Nucleosome-Like Structure with Circular Double-Stranded DNA. *Cell*, 172, pp. 265-274

Rouviere-Yaniv, K. D. a. J. (1987). Histonelike Proteins of Bacteria. *Microbiological review*, 513, pp. 19

Rubinstein, M. & R. H. Colby (2003). Polymer Physics, Oxford University Press.

Sagi, D., N. Friedman, C. Vorgias, A. B. Oppenheim & J. Stavans (2004). Modulation of DNA Conformations through the Formation of Alternative High-Order HU-DNA Complexes. *J. Mol. Biol*, 3412, pp. 419-428

Schafer, D. A., J. Gelles, M. P. Sheetz & R. Landick (1991). Transcription by Single Molecules of RNA Polymerase Observed by Light Microscopy. *Nature*, 352, pp. 444-448

Schlierf, M., H. Li & J. M. Fernandez (2004). The Unfolding Kinetics of Ubiquitin Captured with Single-Molecule Force-Clamp Techniques. *Proc. Natl. Acad. Sci. U S A*, 10119, pp. 7299-7304

Schuler, B., E. A. Lipman & W. A. Eaton (2002). Probing the Free-Energy Surface for Protein Folding with Single-Molecule Fluorescence Spectroscopy. *Nature*, 4196908, pp. 743-747

Segall, D. E., P. C. Nelson & R. Phillips (2006). Volume-Exclusion Effects in Tethered-Particle Experiments: Bead Size Matters. *Phys. Rev. Lett*, 96, pp. 0883061-4

Selvin, P. R. & T. Ha (2008). Single-Molecule Techniques: A Laboratory Manual, Cold Spring Harbor Laboratory Press.

Shin, J.-H., T. J. Santangelo, Y. Xie, J. N. Reeve & Z. Kelman (2007). Archaeal Minichromosome Maintenance (Mcm) Helicase Can Unwind DNA Bound by Archaeal Histones and Transcription Factors. *J. Biol. Chem*, 2827, pp. 4908-4915

Skoko, D., D. Yoo, H. Bai, B. Schnurr, J. Yan, S. M. McLeod, J. F. Marko & R. C. Johnson (2006). Mechanism of Chromosome Compaction and Looping by the Escherichia Coli Nucleoid Protein Fis. *J. Mol. Biol*, 3644, pp. 777-798

Slutsky, M. (2005). Diffusion in a Half-Space: From Lord Kelvin to Path Integrals. *Am. J. Phys*, 734, pp. 308-314

Stavans, J. & A. Oppenheim (2006). DNA-Protein Interactions and Bacterial Chromosome Architecture. *Phys. Biol*, 34, pp. R1-10

Kowalczyk, S. W., Y. A. Grosberg, Y. Rabin & C. Dekker (2011). Modeling the Conductance and DNA Blockade of Solid-State Nanopores. *Nanotechnology*, 2231, pp. 315101

Strick, T., J.-F. Allemand, V. Croquette & D. Bensimon Twisting and Stretching Single DNA Molecules. *Prog. Biophys. Mol. Biol*, 741-2, pp. 115-140

Thanbichler, M., S. C. Wang & L. Shapiro (2005). The Bacterial Nucleoid: A Highly Organized and Dynamic Structure. *J. Cell. Biochem*, 963, pp. 506-521

van Noort, J., S. Verbrugge, N. Goosen, C. Dekker & R. T. Dame (2004). Dual Architectural Roles of HU: Formation of Flexible Hinges and Rigid Filaments. *Proc. Natl. Acad. Sci. U S A*, 10118, pp. 6969-6974

Volpe, G., T. Brettschneider, L. Helden & C. Bechinger (2009). Novel Perspectives for the Application of Total Internal Reflection Microscopy. *Opt. Express*, 1726, pp. 23975-23985

Walther, K. A., J. Bruji, H. Li & J. M. Fernandez (2006). Sub-Angstrom Conformational Changes of a Single Molecule Captured by Afm Variance Analysis. *Biophys. J*, 9010, pp. 3806-3812

Wang, J. C. (1998). Moving One DNA Double Helix through Another by a Type Ii DNA Topoisomerase: The Story of a Simple Molecular Machine. *Q. Rev. Biophys*, 3102, pp. 107-144

Williams, M. C. (2002). Optical Tweezers: Measuring Piconewton Forces, Biophysical Society.

Wong, W. P. & K. Halvorsen (2006). The Effect of Integration Time on Fluctuation Measurements: Calibrating an Optical Trap in the Presence of Motion Blur. *Opt. Express*, 1425, pp. 12517-12531

Xiao, B., R. C. Johnson & J. F. Marko (2010). Modulation of Hu-DNA Interactions by Salt Concentration and Applied Force. *Nucl. Acids Res*, 3818, pp. 6176-6185

Yildiz, A., J. N. Forkey, S. A. McKinney, T. Ha, Y. E. Goldman & P. R. Selvin (2003). Myosin V Walks Hand-over-Hand: Single Fluorophore Imaging with 1.5-Nm Localization. *Science*, 3005628, pp. 2061-2065

Yildiz, A., M. Tomishige, R. D. Vale & P. R. Selvin (2004). Kinesin Walks Hand-over-Hand. *Science*, 3035658, pp. 676-678

Yin, H., R. Landick & J. Gelles (1994). Tethered Particle Motion Method for Studying Transcript Elongation by a Single RNA Polymerase Molecule. *Biophys. J*, 67, pp. 2468-2478

Zimmermann, J. L., T. Nicolaus, G. Neuert & K. Blank (2010). Thiol-Based, Site-Specific and Covalent Immobilization of Biomolecules for Single-Molecule Experiments. *Nat. Protocols*, 56, pp. 975-985

Zurla, C., A. Franzini, G. Galli, D. D. Dunlap, D. E. A. Lewis, S. Adhya & L. Finzi (2006). Novel Tethered Particle Motion Analysis of Ci Protein-Mediated DNA Looping in the Regulation of Bacteriophage Lambda. *J. Phys.: Condens. Matter*, 18, pp. S225-S234

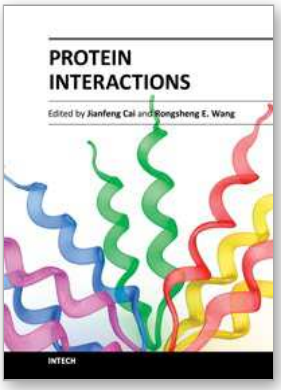

Protein Interactions

Edited by Dr. Jianfeng Cai

ISBN 978-953-51-0244-1
Hard cover, 464 pages
Publisher InTech
Published online 16, March, 2012
Published in print edition March, 2012

Protein interactions, which include interactions between proteins and other biomolecules, are essential to all aspects of biological processes, such as cell growth, differentiation, and apoptosis. Therefore, investigation and modulation of protein interactions are of significance as it not only reveals the mechanism governing cellular activity, but also leads to potential agents for the treatment of various diseases. The objective of this book is to highlight some of the latest approaches in the study of protein interactions, including modulation of protein interactions, development of analytical techniques, etc. Collectively they demonstrate the importance and the possibility for the further investigation and modulation of protein interactions as technology is evolving.

InTech Europe
University Campus STeP Ri
Slavka Krautzeka 83/A
51000 Rijeka, Croatia
Phone: +385 (51) 770 447
Fax: +385 (51) 686 166
www.intechopen.com

InTech China
Unit 405, Office Block, Hotel Equatorial Shanghai
No.65, Yan An Road (West), Shanghai, 200040, China
中国上海市延安西路65号上海国际贵都大饭店办公楼405单元
Phone: +86-21-62489820
Fax: +86-21-62489821